




Grating-based 2D displacement measurement with quadruple optical subdivision of a single incident beam

YUNFEI YIN,^{1,2} ZHAOWU LIU,¹  SHAN JIANG,¹ WEI WANG,¹
HONGZHU YU,¹ WENHAO LI,¹ AND JIRIGALANTU^{1,*}

¹ Changchun Institute of Optics, Fine Mechanics and Physics, Chinese Academy of Sciences, Changchun 130033, China

² University of Chinese Academy of Sciences, Beijing 101408, China

*jiri5998@163.com

Abstract: We propose a new symmetrical heterodyne grating displacement measurement method, based on 2D grating and single diffraction quadruple subdivision method. Using a dual-frequency laser with a wavelength of 632.8 nm, output power of 2.2 mW, and a 1200 l/mm 2D grating, eight diffracted light beams interfere in pairs in the X and Y directions through a turning element. The detection system's measurement accuracy was assessed experimentally. The system measurement resolution in the X and Y directions is better than 3 nm; the grating displacement measurement errors within a 10 mm range are better than ± 30 nm and ± 40 nm, and the repeatability error is better than ± 25 nm. The method is not only applicable to nanoscale 2D displacement measurement technology but also can be used for ultra-precision positioning and ultra-precision processing, with the potential for picometer-level improvement.

© 2021 Optical Society of America under the terms of the [OSA Open Access Publishing Agreement](#)

1. Introduction

Ultra-precision displacement measurement technology plays an important role in the development of semiconductor manufacturing, precision machining, and other fields [1,2]. In recent years, further development of lithography and chip manufacturing, higher demand for measurement precision, dimensions, stability and itinerary. Widely used ultra-precision measurement methods currently include optical fiber sensors, capacitance/inductance micrometers, laser interferometers, and ultra-high precision grating rulers, and each of these approaches has its advantages and limitations. In contrast, the grating interference displacement measurement method based on 2D gratings has the advantage of being an absolute measurement approach [3,4]. In the ultra-precision displacement measurement field, this technique has become increasingly important and also represents the future development trend for ultra-precision measurement technology.

The 2D grating displacement measurement method first appeared in the Netherlands. In 1987, ASML used two orthogonal 1D gratings to realize X- and Z-direction displacement measurements through double optical subdivision. In 1995, the German company Heidenhain manufactured 2D gratings with grid spacing of 8 μm and measurement resolution of 1 nm. In 2009, a 400 mm \times 400 mm 2D grating was applied to the NXT:1950i lithography machine from ASML; accurate positioning was realized through single diffraction and scanning of the grating, and the cumulative machining error of the lithography machine was better than 2.5 nm [5–7]. Therefore, the ultra-precision displacement measurement method based on the 2D grating single diffraction method was actually first applied to ASML lithographic equipment [8] and became the most advanced 2D displacement measurement technology in the world at that time.

At present, the single diffraction method is used widely, with techniques including addition of one way to measure light and use of high-reticle-density gratings [9,10]. In the period from 2007 to 2015, Gao's team [11–17] developed a 2D grating-based single diffraction method to

realize multidimensional surface coding technology by combining four photodetector units with cross-calibration to realize six-dimensional (6D) measurement. From 2011 to 2016, Hsieh's team [18–21] developed the 2D transmission grating-based single diffraction method to realize 3D displacement measurement, and also applied their technology by combining a beam expander with heterodyne modulation to realize 2D grating displacement measurements in a quasi-common optical path. From 2016 to 2019, Tan's team [22–24] used the single diffraction behavior of a 2D grating acting as a beam splitter and refractive element to realize 3D displacement measurements through the measurement grating by combining acousto-optic modulation (AOM) with spatial separation to eliminate the periodic nonlinear errors. In addition, from 2006 to 2012, Fan's team [25–28] realized multidimensional displacement measurements based on 2D grating single diffraction. In 2018, Lin [29] obtained a high signal-to-noise ratio and high contrast using 2D grating diagonally diffracted light. The above-mentioned single diffraction based on 2D gratings is also limited to twice the optical subdivision. This paper develops a single-diffraction four-fold subdivision method, which uses first-order diffracted light to increase the energy utilization rate, and at the same time uses a 2D grating as a reference to detect high-precision 2D displacement information in real time; The integrated design (mechanical structure and optical structure) can reach 35mm×25mm×29 mm. However, different components of different error requirements, increasing the difficulty of integration, may be from the compensation angle to increase the error tolerance.

This paper is based on the heterodyne displacement measurement structure design of the quadruple subdivision of a 2D grating single diffraction. It mainly starts from the principle of the structure design, focusing on the performance and feasibility of the system. Periodic nonlinear errors and 2D grating errors are discussed. Summary of test results by test system, study the significance and progress, further elaborated the future trend of improvement and effective and feasible way.

2. Measurement principle

The displacement measuring system based on 2D gratings, often simplified to two 1D displacement measurements, while ignoring the unusual properties of 2D gratings. To improve the practicality of the real-time measurement of 2D gratings and also satisfy the demand for high precision and multidimensional measurements, this paper proposes a 2D grating-based symmetric heterodyne grating displacement measurement system, as illustrated in Fig. 1. A dual-frequency laser emits a beam of linearly polarized light perpendicular to the system's small axis (with frequencies f_1 and f_2) that is divided into two beams by the polarizing splitter beam (PBS) prism; the reflected light (f_1) is emitted through plane mirror (M), and the transmitted light (f_2) is emitted through the square retroreflector. These beams are then simultaneously incident on the 2D grating via the PBS and form eight diffracted light beams; f_1 : (+1,0), (−1,0), (0,+1), and (0,−1); f_2 : (+1,0), (−1,0), (0,+1), and (0,−1). where the diffracted light of order (+1,0) at frequency f_1 is reflected by the turning element, the quarter-wave plate (QWP), and the PBS, and after transmission and reflection twice by the QWP and the square retroreflector, is then transmitted through the PBS and is incident on the fiber coupler 1x. The diffracted light of order (−1,0) of frequency f_2 passes through the turning element and the QWP, is transmitted by the PBS, reflected by the QWP and M, reflected by the PBS, and is then incident into the fiber coupler 1x; the measurement signal I_{1x} can then be obtained;

where the diffracted light of order (−1,0) at frequency f_1 is reflected by the turning element, QWP, and PBS, and after transmission and reflection twice by the QWP and the square retroreflector, is then transmitted through the PBS and is incident on the fiber coupler 1y. The diffracted light of order (+1,0) of frequency f_2 passes through the turning element and the QWP, is transmitted by the PBS, reflected by the QWP and M, reflected by the PBS, and is then incident into the fiber coupler 1y; the measurement signal I_{1y} can then be obtained;

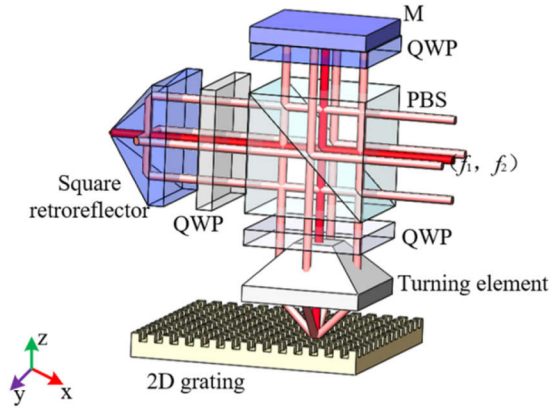


Fig. 1. Schematic diagram of the proposed displacement measurement method using the symmetrical heterodyne grating.

where the diffracted light of order $(0, -1)$ at frequency f_1 is reflected by the turning element, QWP, and the PBS, and after transmission and reflection twice by the QWP and the square retroreflector, is then transmitted through the PBS and is incident on the fiber coupler $2x$. The diffracted light of order $(0, +1)$ of frequency f_2 passes through the turning element and the QWP, is transmitted by the PBS, reflected by the QWP and M, reflected by the PBS, and is then incident into the fiber coupler $2x$; the measurement signal I_{2x} can then be obtained;

where the diffracted light of order $(0, +1)$ at frequency f_1 is reflected by the turning element, QWP, and PBS, and after transmission and reflection twice by the QWP and the square retroreflector, is then transmitted through the PBS and is incident on the fiber coupler $2y$. The diffracted light of order $(0, -1)$ of frequency f_2 passes through the turning element and the QWP, is transmitted by the PBS, reflected by the QWP and M, reflected by the PBS, and is then incident into the fiber coupler $2y$; the measurement signal I_{2y} can then be obtained;

The displacement measurement system realizes the real-time displacement measurements in the X and Y directions using an electrical process; in the actual experiment, the turning element is replaced with four planar mirrors.

In combination with the literature [4], the principle of the proposed displacement measurement method using the symmetric heterodyne grating is derived, where the output signal from the dual-frequency laser can be expressed as follows:

$$E_0 = \begin{bmatrix} 1 \\ 0 \end{bmatrix} \exp[i(2\pi f_1 t + \varphi_1)] + \begin{bmatrix} 0 \\ 1 \end{bmatrix} \exp[i(2\pi f_2 t + \varphi_2)] \quad (1)$$

where f_1 and f_2 represent the initial frequencies of the two orthogonal linearly polarized beams, and φ_1 and φ_2 denote the initial phases of these two beams, respectively. The reference signal of the incident laser beam can then be expressed as:

$$I_r \propto \cos[2\pi(f_1 - f_2)t + \varphi_1 - \varphi_2] \quad (2)$$

When the interference light is incident on the optical fiber coupler, the detected energies I_{1x} , I_{1y} , I_{2x} and I_{2y} in the optical fiber coupler can be expressed as follows:

$$I_{1x} \propto |E_{r_{1,0}} + E_{r_{-1,0}}|^2 \propto \cos[2\pi(f_1 - f_2 + 2\Delta f)t + (\varphi_1 - \varphi_2) + 2\phi] \quad (3)$$

$$I_{2x} \propto |E_{r_{-1,0}} + E_{r_{1,0}}|^2 \propto \cos[2\pi(f_1 - f_2 - 2\Delta f)t + (\varphi_1 - \varphi_2) - 2\phi] \quad (4)$$

$$I_{1y} \propto |E_{r_{0,+1}} + E_{r_{0,-1}}|^2 \propto \cos[2\pi(f_1 - f_2 + 2\Delta f)t + (\varphi_1 - \varphi_2) + 2\phi] \quad (5)$$

$$I_{2y} \propto |E_{r_{0,-1}} + E_{r_{0,1}}|^2 \propto \cos[2\pi(f_1 - f_2 - 2\Delta f)t + (\varphi_1 - \varphi_2) - 2\phi] \quad (6)$$

where Δf is the Doppler frequency shift caused by the displacement of the 2D grating; ϕ is the phase shift caused by the diffracted light on the plane of the 2D grating, and the phase changes can be expressed as follows:

$$\phi_{(1x,0)} = \Delta\varphi + \frac{4\pi}{d_x}\Delta x - \frac{4\pi}{d_y}\Delta y \quad (7)$$

$$\phi_{(-1x,0)} = \Delta\varphi - \frac{4\pi}{d_x}\Delta x - \frac{4\pi}{d_y}\Delta y \quad (8)$$

$$\phi_{(0,1y)} = \Delta\varphi + \frac{4\pi}{d_x}\Delta x + \frac{4\pi}{d_y}\Delta y \quad (9)$$

$$\phi_{(0,-1y)} = \Delta\varphi + \frac{4\pi}{d_x}\Delta x - \frac{4\pi}{d_y}\Delta y \quad (10)$$

Selection of the 1200 l/mm grating maintains a consistent grating pitch in both the X- and Y-directions, and d represents the grating constant, where $d_x = d_y$; Δx and Δy denote the displacements of the 2D grating along the X- and Y-directions during the process of motion; and $\Delta\varphi = \varphi_1 - \varphi_2$ is the initial phase difference of the initial laser beam. The interference light that enters the electronic device module can be subtraction processed, the distances moved by the 2D grating in the X- and Y-directions can be expressed as follows:

$$\Delta x = \frac{d_x}{8\pi} \Delta\phi_{(x)} \quad (11)$$

$$\Delta y = \frac{d_y}{8\pi} \Delta\phi_{(y)} \quad (12)$$

Analysis of Eqs. (13) and (14) indicates that the measurement signals for the X- and the Y-direction can either be measured separately or measured in real time with two axes, and directional discrimination analysis of the X- and Y-directions can thus be realized.

3. Experimental testing

3.1. Experimental setup

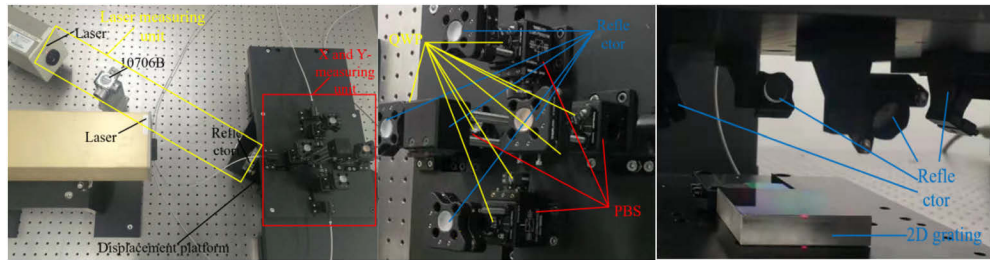


Fig. 2. Schematic of the 2D displacement measurement test apparatus: a) schematic view of the overall configuration of the experimental device; b) schematic of the X and Y displacement measurement grating; c) schematic of the turning element for the X and Y displacement measurements.

The feasibility of the test system is verified using an orthogonal linear polarization He-Ne laser with a transmission direction of 45° , laser power of 2.2 mW, and stability of less than 5% (Model: DH-HN250) as the light source. A long-stroke displacement platform with a 300 mm stroke (Model: XML210) is used as a mobile structure. A long-stroke displacement flotation stage and isolation platform was placed in 60° , not only 2D motion can be achieved, and can be achieved simultaneously detecting X and Y displacement values. In this experiment, as shown in Fig. 2, a reflective 2D grating with a high groove density (period: 833.3 nm; range up grating with dimensions of 68 mm \times 68 mm, where the 2D diffraction efficiencies in the X and Y directions are 18% and 21%, respectively) made via holographic technology is used, and this 2D grating is installed on an optical isolation flotation platform (XM-S). Two dual-frequency lasers are used, where one is used for the detection part of the laser interferometer control group, and the other is used for the detection part of the heterodyne grating displacement measurement system to realize real-time precision measurement of the 2D displacement in the X and Y directions. The clean room laboratory temperature is restricted to $21^\circ\text{C} \pm 0.05^\circ\text{C}$.

3.2. Linear displacement measurement

To demonstrate the feasibility of the single optical diffraction-based quadruple subdivision scheme based on a 2D grating, a square retroreflector, and the phase decoupling method, the 10705B interferometer was used to perform linear displacement experiments in the X- and Y-directions. The displacement table was made to move along at an angle of 30° , and the measurement results for the X-direction linear displacement of the measuring system are as shown in Fig. 3. The displacement table was then made to move along at an angle of -150° , and the measurement results for the Y-direction linear displacement of the measuring system are as shown in Fig. 4. The experiments showed that the displacement change values for the X- and Y-direction displacement measurement system based on the 2D grating were 10.0020 mm and 10.0024 mm, and the X- and Y-direction displacement changes based on the laser wavelength were 10.0010 mm and 10.0020 mm, respectively. The causes of the differences in these results are the influence of air disturbances in the environment and the different spectral efficiencies of the devices used; according to the fluctuations in the linear error value, for linear movement within a 10 mm range, the linear errors caused by the grating displacement measurement system are ± 30 nm and ± 40 nm for the X- and Y-directions, respectively. These results confirm that the proposed grating displacement measurement system has a good linear measurement capability.

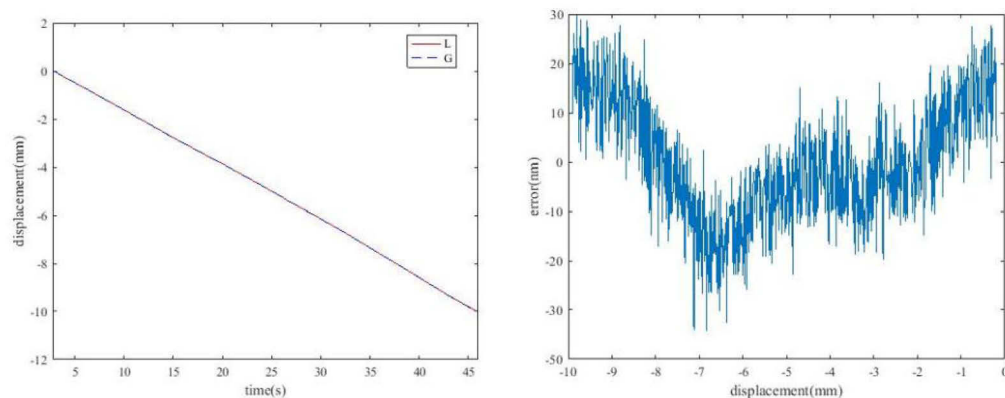


Fig. 3. X-direction linear displacement measurement results from the measuring system: a) linear displacement measurements; b) linear measurement error fluctuations.

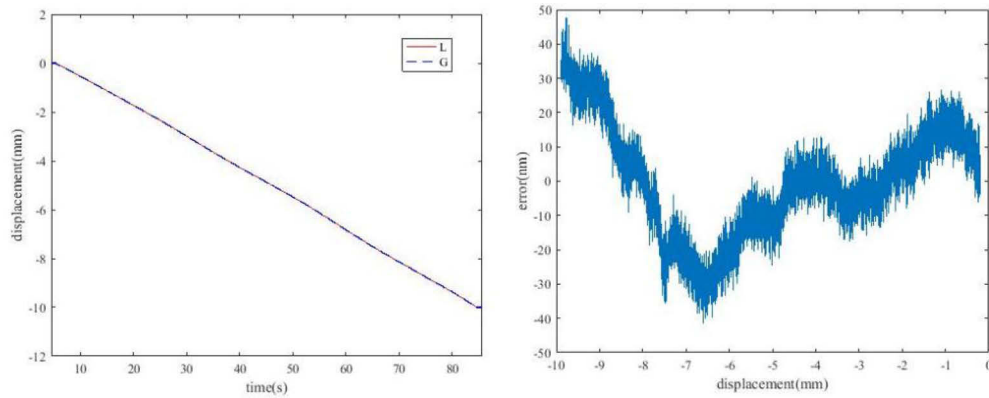


Fig. 4. *Y*-direction linear displacement measurement results from the measuring system: a) linear displacement measurements; b) linear measurement error fluctuations.

3.3. Measurement repeatability

Repeatability testing is the main indicator of the accuracy of the grating displacement measurement system. To prove the repeatability of the changes and the mutual influence of the displacements in the *X*- and *Y*-directions during the measurements, it is necessary to maintain the levels of influence in the two directions as consistently as possible. Experiments show that when the mobile platform is driven in a linear direction with a back and forth movement of 2 mm, the measurement results for the proposed grating displacement measurement system in the *X*- and *Y*-directions are 1.995 mm and 2.000 mm, as shown in Figs. 5 and 6, respectively. Comparison tests using the laser interferometer for the case of four-round repeatability in the *X*- and *Y*-directions showed that the errors of the grating displacement measuring system along the *X*-direction over two periods were maintained within ± 30 nm, and the errors of the grating displacement measurement system along the *Y*-direction over four periods were maintained within ± 25 nm. These results show that our proposed grating displacement measurement system provides better reproducibility and that its repeatability error remains constant.

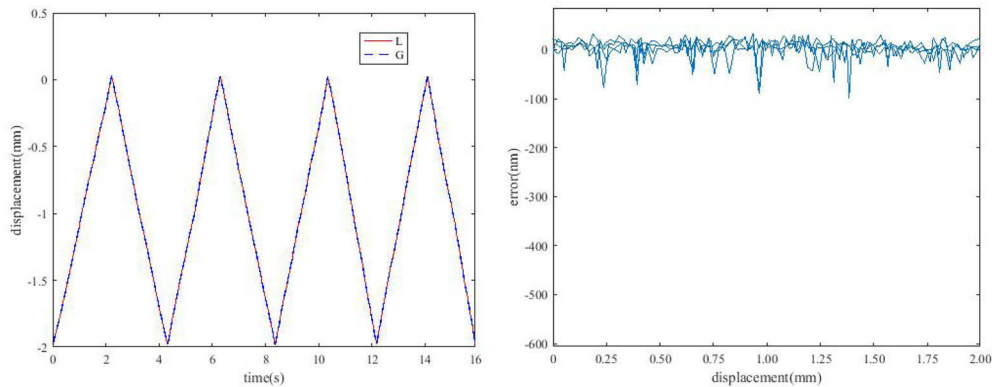


Fig. 5. Measurement results for *X*-direction repeatability of the measuring system: a) four-round repeatability test; b) error change within two periods.

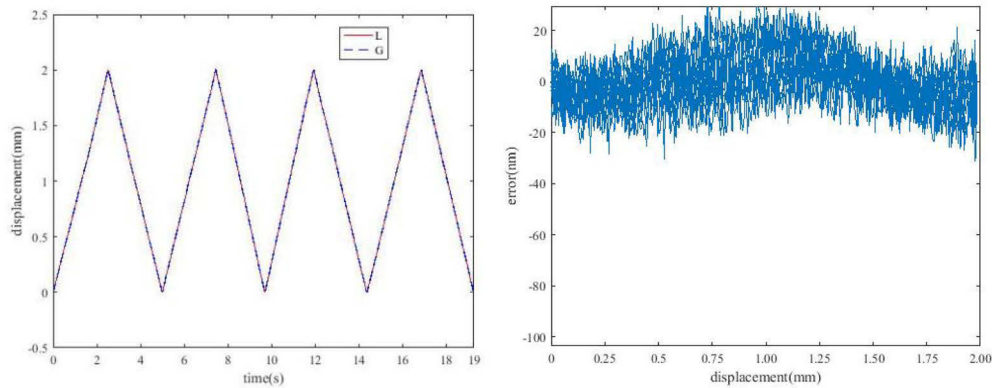


Fig. 6. Measurement results for Y-direction repeatability of the measuring system: a) four-round repeatability test; b) error change within four periods.

3.4. Nanometer-range measurements

The displacement measurement system based on the 2D grating and the single diffraction quadruple subdivision method in the X- and Y-directions can achieve a measurement resolution of 0.203 nm. To prove that the grating displacement measurement system has a high accuracy displacement measurement capability, the displacement table was used to generate displacement values of 15 nm and 24 nm with a step size of 3 nm, with results as shown in Figs. 7 and 8. The experiments showed that the actual resolution of the proposed grating displacement measuring system is better than 3 nm; the laser displacement measurement system error was maintained substantially within the ± 2 nm range, the grating displacement measuring system error was maintained within the ± 5 nm range at the step size of 3 nm, and difference calculations were performed. The results show that the changes in the X-direction 3σ values of the laser interferometer and grating displacement measurement systems are 3.278 nm, 3.934 nm, and 4.262 nm, and 5.245 nm, 5.573 nm, and 5.282 nm, respectively; the changes in the Y-direction 3σ values of the laser

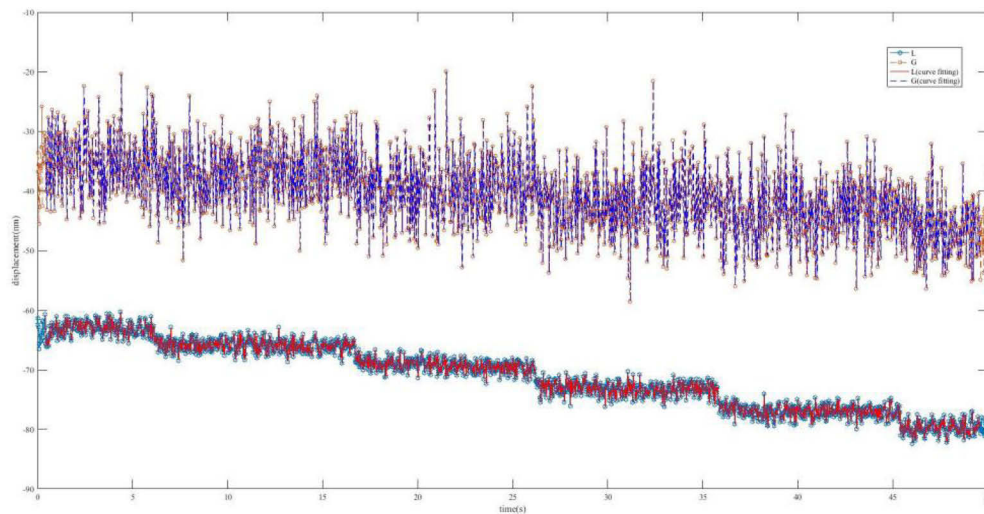


Fig. 7. Measurement results for the X-direction nanometer range of the measurement system.

interferometer and grating displacement measurement systems are 4.891 nm, 5.179 nm, and 6.042 nm, and 6.905 nm, 6.042 nm, and 6.258 nm, respectively. These results indicate that the grating displacement measurement system errors mainly come from air disturbance errors from the external environment, and polarization aliasing of the device also introduces nonlinear errors. These results therefore demonstrate that our proposed grating displacement measuring system has the ability to resolve nanometer-scale displacement measurements.

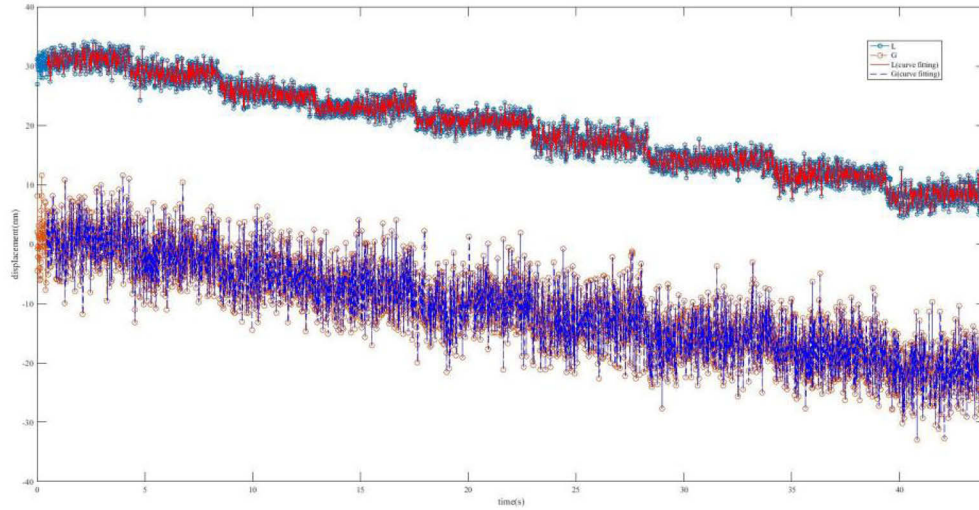


Fig. 8. Measurement results for the *Y*-direction nanometer range of the measurement system.

4. Discussion

The proposed grating displacement measurement system is based on the 2D grating pitch, combined with a heterodyne structure design. The system error sources for grating displacement measurement are mainly nonlinear errors introduced by polarization aliasing of the devices and disturbance errors introduced by angle migration of the 2D grating. In the following, detailed analyses of the two types of error are presented.

4.1. Nonlinear error

Generally, Reducing the nonlinear error introduced by the polarization component can: high-groove-density gratings, symmetrical grating structure design, and separate structural design. In this experiment, the main error is introduced into the PBS by mixing two types of polarization from the PBS and the QWP, which causes the azimuth angle to change and results in a phase delay.

When the PBS and the *X*-axis produce a small angle θ_1 , the measurement beam can be expressed as:

$$E = P(\theta_1) \frac{1}{4} \sin(2\alpha) H(\delta_1) \{ \exp[i(2\pi f_1 t + \varphi_1)] + \exp[i(2\pi f_2 t + \varphi_2)] \} \quad (13)$$

where θ_1 is the polarization angle introduced by the offset, α is the angular deviation introduced by the PBS misalignment, and δ_1 is the phase delay introduced by incomplete registration. The

interference signal can be expressed as follows:

$$I_1 \propto |E|^2 \propto \cos[2\pi(f_1 - f_2)t + (\varphi_1 - \varphi_2 + 2\varphi_{(\delta_1, \alpha, \theta_1)})] \quad (14)$$

$$\Delta\varphi = \varphi_1 - \varphi_2 + 2\varphi_{(\delta_1, \alpha, \theta_1)} \quad (15)$$

When the PBS and the QWP are aliased together, the interference amplitude can be expressed as:

$$E = P(\theta_1, \theta_2) \begin{bmatrix} \frac{1}{4} \sin 2\alpha \\ i \frac{1}{4} \sin 2\alpha \sin 2\beta \end{bmatrix} H(\delta_1, \delta_2) \{ \exp[i(2\pi f_1 t + \varphi_1)] + \exp[i(2\pi f_2 t + \varphi_2)] \} \quad (16)$$

According to the superposition effect, $\theta_2 = \theta_1 + \Delta\theta$ and $\delta_2 = \delta_1 + \Delta\delta$, where $\Delta\theta$ is the polarization bias of the polarized light passing through the PBS; $\Delta\delta$ is the phase delay error caused by the QWP, θ_2 is the deviation between the polarization angles of the PBS and the QWP, δ_2 is the phase delay after incomplete alignment of the PBS and the QWP, and β is the angular deviation introduced by misalignment of the QWP. The interference signal can then be expressed as:

$$I_1 \propto |E|^2 \propto \cos[2\pi(f_1 - f_2)t + (\varphi_1 - \varphi_2 + 2\varphi_{(\delta_1, \alpha, \theta_1)})] + \cos[2\pi(f_1 - f_2)t + (\varphi_1 - \varphi_2 + 2\varphi_{[\delta_2, (\alpha, \beta), \theta_2]})] + \Delta \quad (17)$$

where (α, β) is the angular deviation caused by co-aliasing, and the deviation amplitude is $1/4 \sin 2\alpha \sin 2\beta$; Δ is the multiplied tiny number under the influence of the first two items, but because the amount of variation is a higher-order term, it can be ignored numerically.

Here,

$$\Delta\varphi = 2(\varphi_1 - \varphi_2) + 2\varphi_{(\delta_1, \alpha, \theta_1)} + 2\varphi_{[\delta_2, (\alpha, \beta), \theta_2]} \quad (18)$$

In the experiments, the PBS and the QWP are controlled to within 40'' and 2' using a precision rotary mount, where the yaw angle error is controlled to within 4' and 2' by the ultra-precision mounting bracket, respectively; the angle deviation introduced by the polarized light is 8' 24'', where the angles of deviation caused by the PBS and the QWP are 2'' and 42'', respectively. Figure 9 shows that the amplitude changes caused by the nonlinear errors introduced by the PBS are 0.650, 0.845; and 0.916, and the analysis shows that when the polarized light moves slightly, the nonlinear errors caused by this movement of the measurement system cannot be ignored. The amplitude changes caused by the nonlinear errors introduced by the PBS and the QWP are 1.670, 1.620, 1.412 and 0.876, and the analysis shows that when a symmetrical structure distribution is used, the polarization aliasing error tends to remain stable. However, because the small angle deviation of the polarized light cannot be ignored, the correction can be performed by interferometric measurement of two symmetrical beams of light in the same optical path, 2D gratings with high-groove-density can also be used.

4.2. Disturbance error of 2D grating

(a) Yaw angle (θ_x)

When an offset is generated about the X-axis, X-axis, Y-axis, and Z-axis detection errors are also introduced. According to the measurement principle, the diffracted light will have an angular difference of two times the yaw angle. When this difference is measured along the X-axis, the Y-axis and the Z-axis are driven simultaneously, and their changes in yaw (Δl_{yaw}) can be

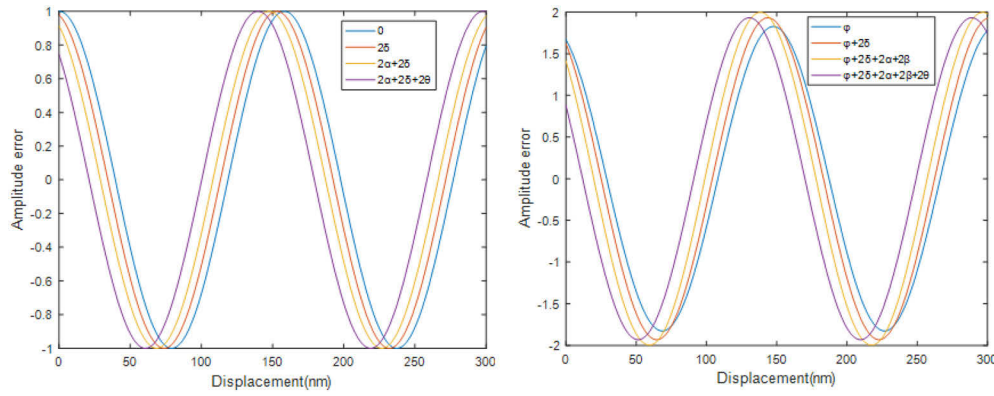


Fig. 9. Nonlinear errors: (a) PBS aliasing errors; (b) aliasing errors under the action of the PBS and the QWP.

expressed as:

$$\Delta l_{yawY} = \frac{\Delta\varphi}{4\pi}(l - l_{yaw}) = \Delta l \left(\frac{1}{\cos \theta_x} - 1 \right) \quad (19)$$

$$\Delta l_{yawZ} = \frac{\Delta\varphi}{4\pi}(l - l_{yaw}) = \Delta l(\tan \theta_x - 1) \quad (20)$$

where θ_x represents the change in the yaw angle caused by motion around the X -axis, and Δl indicates the magnitude of the yaw misalignment impact. In the measurements, the variation in the Z -axis measurement results is mainly caused by yaw. When measured along the direction of Y -axis movement, which causes changes in the height along the Z -axis and the grating line width of the X -axis, the changes in the yaw (Δl_{yaw}) can be expressed as:

$$\Delta l_{yawY} = \frac{\Delta\varphi}{4\pi}(l - l_{yawY}) = \Delta l(1 - \cos \theta_x) \quad (21)$$

$$\Delta l_{yawZ} = \frac{\Delta\varphi}{4\pi}(l - l_{yawZ}) = \Delta l(\tan \theta_x - \sin \theta_x) \quad (22)$$

where the changes along the Y -axis and the Z -axis are determined by the yaw angle of the change in verticality caused by the movement of the 2D grating, and Δl_{yawY} and Δl_{yawZ} are the amounts of yaw produced when moving along the Y -axis and the Z -axis, respectively.

b) Pitch angle (θ_y)

When pitching is generated about the Y -axis, X -axis, Y -axis, and Z -axis detection errors are also introduced; according to the measurement principle, the diffracted light will have an angular difference of two times the pitch angle. When the pitch is measured along the Y -axis, the X -axis and the Z -axis are driven simultaneously, and the changes in pitch (Δl_{pitch}) can be expressed as:

$$\Delta l_{pitchX} = \frac{\Delta\varphi}{4\pi}(l - l_{pitch}) = \Delta l \left(\frac{1}{\cos \theta_y} - 1 \right) \quad (23)$$

$$\Delta l_{pitchZ} = \frac{\Delta\varphi}{4\pi}(l - l_{pitch}) = \Delta l(\tan \theta_y - 1) \quad (24)$$

where θ_y represents the change in the pitch angle caused by movement around the X -axis and Δl indicates the magnitude of the pitch misalignment impact. During the measurements, the variations in the Z -axis measurement results are mainly caused by the pitch; when measured

along the X -axis movement, it causes the height change of the Z -axis and the grating line width of the Y -axis grating to change, and these changes in pitch (Δl_{pitch}) can be expressed as:

$$\Delta l_{pitchY} = \frac{\Delta\varphi}{4\pi}(l - l_{pitchY}) = \Delta l(1 - \cos\theta_y) \quad (25)$$

$$\Delta l_{pitchZ} = \frac{\Delta\varphi}{4\pi}(l - l_{pitchZ}) = \Delta l(\tan\theta_y - \sin\theta_y) \quad (26)$$

where the changes along the Y -axis and the Z -axis are determined by the pitching angle of the 2D grating movement with respect to the change in perpendicularity, and Δl_{yawY} and Δl_{yawZ} are the amounts of pitch produced when moving along the Y -axis and the Z -axis, respectively. Because of the change in the width of the grating line, according to the grating equation, $n\sin\theta_{mn}\cos\Phi_{mn} = \sin\theta\cos\Phi + m\lambda/d$, but when the grating pitch changes slightly, $\theta = \arcsin[\lambda/(d + \Delta d)(n_l - 1)]$, and although this angle change is negligible, it introduces a change in the height along the Z -axis.

c) Roll angle (θ_z)

When rolling is generated about the Z -axis, because the light path of the Z -axis remains unchanged, roll errors will be introduced to the X -axis and the Y -axis; both roll errors are the same and can be expressed as follows:

$$\Delta l_{rollX} = \Delta l_{rollY} = \frac{\Delta\varphi}{4\pi}(l - l_{roll}) = \tan\theta_z\{\Delta l[\cos(\Delta\theta_z)] - \cos[\Delta\theta_z + \Delta\theta'_z]\} \quad (27)$$

where $\Delta\theta_z$ and $\Delta\theta'_z$ represent the changes in the rotation angle and the angular offset of the 2D grating line that occur when the roll angle changes, respectively, and l_{roll} represents the deviation of the pitch misalignment by the change in the roll angle.

Figure 10 shows that, when moving along the X -axis and the Y -axis, the 2D grating pitch produces slight variations in both the X -axis and the Y -axis, where the X -axis roll and Y -axis roll quantities are equal, i.e., $\Delta l_{rollX} = \Delta l_{rollY}$. The Z -axis roll quantity is Δl_{rollZ} , and the slight angular variation caused by the grating pitch is θ_z ; when two diffracted light beams exit the surface, the angle of diffraction is α , the initial distance is l_1 , and the spacing between the two diffracted light beams is l_2 . The red dashed line represents the 2D grating light emission in the two positions

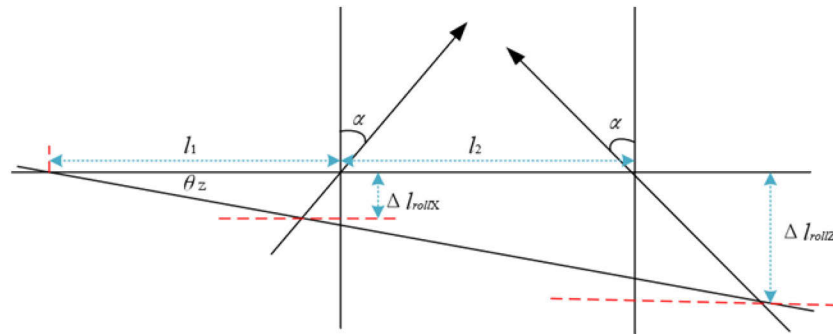


Fig. 10. Schematic diagram of the changes along the X -axis and the Z -axis caused by rolling of the 2D grating.

above, and the amounts of roll along the X-axis and the Z-axis can be expressed as:

$$\Delta l_{rollX} = \frac{l_1 \tan \theta_z}{\tan \theta_z \tan \alpha + 1} \quad (28)$$

$$\Delta l_{rollZ} = \frac{(l_1 + l_2) \tan \theta_z}{1 - \tan \theta_z \tan \alpha} \quad (29)$$

Therefore, the changes in the roll errors along the X-axis and the Y-axis are related to the initial distance, while the change in that along the Z-axis is related not only to the initial distance, but also to the spacing of the diffracted light beams.

5. Conclusion

This paper proposes a symmetric heterodyne grating displacement measurement method based on a single diffraction quadruple subdivision method combining 2D grating, square retroreflector, and phase decoupling. This method combines heterodyne measurement, and the single-phase decoupling method subdivision diffracted four times, using 1200 //mm 2D grating to achieve real-time 2D displacement to the X- and Y-direction precision measurement, gain further potential to use corner prisms for misalignment experiments, fiber gratings, and change the incident method. The feasibility and performance of the proposed heterodyne grating displacement measurement method can be verified through the linear displacement measurement experiment, repeatability measurement experiment and nano measurement experiment. These experiments showed that the theoretical 2D grating displacement measurement resolution of the system ranged up to 0.203 nm, the experimental resolution was better than 3 nm, the grating displacement measurement errors in the X and Y ranges over 10 mm were better than ± 30 nm and ± 40 nm, respectively, and the repeatability error was better than ± 25 nm. In addition, analysis of the polarization of each device and the 2D grating aliasing triaxial system disturbance on the measurement. The test results of this measurement system are better than commercial interferometers, with a wider range of applications and value. The results show that the proposed heterodyne grating displacement measurement structure is very suitable for nanometer-scale displacement measurement. The optical path symmetrical to each other, the principle of a simple and convenient configuration, meets the stability, reliability, and strong anti-interference capability requirements for 2D grating displacement measurement applications.

Additionally, the heterodyne grating displacement measurement system designed here can achieve the same optical path length for the two interfering beams by compensating their optical paths. These paths may also be compensated in real time in the measurement arm and the reference arm to reduce the periodic nonlinear errors introduced by the measurement system which may improve the performance of the test grating, e.g, the 2D grating or holographic exposure copying and splicing stroke will be increased. Extension of the proposed system to multidimensional measurements has also been considered, including integration of the three angular measurements and the three displacement measurements. In particular, longer strokes lead to reduced accuracy in the grating displacement measurement system, which means that it will be necessary to consider the stroke length when compensating the measurement system.

Funding. National Natural Science Foundation of China (62075216); Guangdong Province Key Field R&D Program (2019B010144001); Jilin Province Science and Technology Innovation Project of China (20190201021JC).

Acknowledgments. The author sincerely thanks researchers Jirigalantu and Li Wenhao of Changchun Institute of Optics, Fine Mechanics and Physics for their help and support.

Disclosures. The authors declare no conflicts of interest.

Data availability. Data underlying the results presented in this paper are not publicly available at this time but may be obtained from the authors upon reasonable request.

References

1. Y. Bai, P. C. Hu, Y. F. Lu, Z. K. Li, Z. H. Zhang, and J. B. Tan, "A six-axis heterodyne interferometer system for joule balance," *IEEE Trans Instrum Meas* **66**(6), 1579–1585 (2017).
2. Y. Hori, S. Gonda, Y. Bitou, A. Watanabe, and K. Nakamura, "Periodic error evaluation system for linear encoders using a homodyne laser interferometer with 10 picometer uncertainty," *Precision Engineering* **51**, 388–392 (2018).
3. J. L. Deng, X. N. Yan, C. L. Wei, Y. C. Lu, M. K. Li, X. S. Xiang, W. Jia, and C. H. Zhou, "Eightfold optical encoder with high-density grating," *Applied Optics* **57**(10), 2366–2375 (2018).
4. Q. Lv, Z. W. Liu, W. Wang, X. Li, S. Li, Y. Song, H. Z. Yu, H. X. G. Bayin, and W. H. Li, "Simple and compact grating-based heterodyne interferometer with the Littrow configuration for high-accuracy and long-range measurement of two-dimensional displacement," *Applied Optics* **57**(31), 9455–9463 (2018).
5. Y. F. Yin, Z. W. Liu, G. L. T. Jiri, H. Z. Yu, W. Wang, X. T. Li, H. Bao, W. H. Li, and Q. Hao, "Overview of 2D grating displacement measurement technology," *Chinese Optics* **13**(6), 1224–1238 (2020).
6. P. C. Hu, D. Chang, J. B. Tan, R. T. Yang, H. X. Yang, and H. J. Fu, "Displacement measuring grating interferometer: a review," *Frontiers of Information Technology & Electronic Engineering* **20**(5), 631–654 (2019).
7. E. A. F. Vander and E. R. Loopstra, "Position measurement unit, measurement system and lithographic apparatus comprising such position measurement unit," P. U.S Patent 7,362,446, 22(4) (2008).
8. T. Castenmiller, V. D. M. Frank, and D. K. Toine, "Towards ultimate optical lithography with NXT: 1950i dual stage immersion platform," *Proceedings of SPIE* **76401N**, 76401N (2010).
9. Z. Tao, J. W. Cui, and J. B. Tan, "Simultaneous multi-channel absolute position alignment by multi-order grating interferometry," *Optics Express* **24**(2), 802–816 (2016).
10. J. Guan, P. Kochert, C. Weichert, R. Koning, L. Siaudinyte, and J. Flugge, "A differential interferometric heterodyne encoder with 30 picometer periodic nonlinearity and sub-nanometer stability," *Precis. Eng.* **50**, 114–118 (2017).
11. W. Gao and A. Kimura, "A three-axis displacement sensor with nanometric resolution," *CIRP Annals* **56**(1), 529–532 (2007).
12. A. Kimura, W. Gao, Y. Arai, and L. Zeng, "Design and construction of a two-degree-of-freedom linear encoder for nanometric measurement of stage position and straightness," *Precision Engineering* **34**(1), 145–155 (2010).
13. A. Kimura, W. Gao, and L. Zeng, "Position and out-of-straightness measurement of a precision linear air-bearing stage by using a two-degree-of-freedom linear encoder," *Meas. Sci. Technol.* **21**(5), 054005 (2010).
14. A. Kimura, W. Gao, W. J. Kim, K. Hosono, Y. Shimizu, L. Shi, and L. Zeng, "A sub-nanometric three-axis surface encoder with short-period planar gratings for stage motion measurement," *Precision Engineering* **36**(4), 576–585 (2012).
15. W. Gao, Y. Saito, H. Muto, Y. Arai, and Y. Shimizu, "A three-axis autocollimator for detection of angular error motions of a precision stage," *CIRP Annals* **60**(1), 515–518 (2011).
16. X. H. Li, W. Gao, H. Muto, Y. Shimizu, S. Ito, and S. Dian, "A six-degree-of-freedom surface encoder for precision positioning of a planar motion stage," *Precision Engineering* **37**(3), 771–781 (2013).
17. W. Gao, S. W. Kim, H. Bosse, H. Haitjema, Y. L. Chen, X. D. Lu, W. Knapp, A. Weckenmann, W. T. Estler, and H. Kunzmann, "Measurement technologies for precision positioning," *CIRP Annals* **64**(2), 773–796 (2015).
18. H. L. Hsieh, J. C. Chen, G. Lerondel, and J. Y. Lee, "Two-dimensional displacement measurement by quasi-common-optical-path heterodyne grating interferometer," *Optics Express* **19**(10), 9770–9782 (2011).
19. H. L. Hsieh and S. W. Pan, "Three-degree-of-freedom displacement measurement using grating-based heterodyne interferometry," *Applied Optics* **52**(27), 6840–6848 (2013).
20. H. L. Hsieh and S. W. Pan, "Development of a grating-based interferometer for six-degree-of-freedom displacement and angle measurements," *Optics Express* **23**(3), 2451–2465 (2015).
21. H. L. Hsieh and W. Chen, "Heterodyne wollaston laser encoder for measurement for in-plane displacement," *Optics Express* **24**(8), 8693 (2016).
22. P. P. Wei, X. Lu, D. C. Qiao, L. M. Zou, X. D. Huang, J. B. Tan, and Z. G. Lu, "Two-dimensional displacement measurement based on two parallel gratings," *Rev. Sci. Instrum.* **89**(6), 065105 (2018).
23. Z. G. Lu, P. P. Wei, C. Q. Wang, J. L. Jing, J. B. Tan, and X. P. Zhao, "Two-degree-of-freedom displacement measurement system based on double diffraction gratings," *Meas. Sci. Technol.* **27**(7), 074012 (2016).
24. X. Xing, D. Chang, P. C. Hu, and J. B. Tan, "Spatially separated heterodyne grating interferometer for in-plane displacement measurement," *Optics and Precision Engineering* **27**(8), 1727–1736 (2019).
25. K. C. Fan, Y. S. Liu, Y. J. Chen, and F. Cheng, "A linear diffraction grating interferometer with high accuracy," *Proceedings of SPIE* **6280**, 628008 (2006).
26. C. F. Kao, S. H. Lu, H. M. Shen, and K. C. Fan, "Diffraction laser encoder with a grating in Littrow configuration," *Jpn. J. Appl. Phys.* **47**(3), 1833–1837 (2008).
27. Y. C. Chung, K. C. Fan, and B. C. Lee, "Development of a novel planar encoder for 2D displacement measurement in nanometer resolution and accuracy," *J. Proceedings of the World Congress on Intelligent Control and Automation (WCICA)*:449–453 (2011).
28. K. C. Fan, Y. L. Zhang, J. W. Miao, and F. Cheng, "Error compensation of grating interferometer due to angular error of linear stage," *J. IEEE/ASME International Conference on Advanced Intelligent Mechatronics, AIM*, 428–431 (2012).
29. C. B. Lin, S. H. Yan, D. Ding, and G. C. Wang, "Two-dimensional diagonal-based heterodyne grating interferometer with enhanced signal-to-noise ratio and optical subdivision," *Opt. Eng.* **57**(06), 1 (2018).